Energy loss of slow carbon cluster ions in thin carbon foils

Yasuyuki Takahashi,* Toshiyuki Hattori, and Noriyosu Hayashizaki
Research Laboratory for Nuclear Reactors, Tokyo Institute of Technology, 2-12-1, O-okayama, Meguro-ku, Tokyo 152-8550, Japan
(Received 10 July 2004; revised manuscript received 17 October 2006; published 9 January 2007)

We have investigated the nonlinear effects in the stopping power of carbon cluster ions propagating through a thin carbon foil at some velocities lower than the Bohr velocity. We measured the energy loss of slow C_n^+ $(2 \leqslant n \leqslant 21)$ cluster ions passing through carbon foils of 1.0–10.0 $\mu g/cm^2$ in thickness at energies of 1.5–40 keV/atom. For all incidents of C_n^+ $(2 \leqslant n \leqslant 21)$ cluster ions, we observed few but rigid amount of intact cluster ions with 3.3%–19.5% reduced in energy but with no atomic loss after passing through a thin 1.0 $\mu g/cm^2$ carbon foil. The stopping power ratios defined as the stopping power per atom of cluster ions divided by the stopping power of isolated atomic ions at the same velocity were evaluated using a simplified united-atom model as well as an experimental approach. The stopping power ratios of the intact cluster ions in all cluster sizes were much smaller than unity. The authors found the remarkable nonlinear effects in the low-energy region to be contrary to those predicted previously for the stopping power of the cluster ions.

DOI: 10.1103/PhysRevA.75.013202 PACS number(s): 36.40.−c, 34.50.Bw, 39.10.+j

I. INTRODUCTION

The various phenomena associated with interactions of molecular ions and cluster ions with solids have proven to be interesting research subjects in recent years. The molecular and cluster ion impact exhibits multiple atomic collisions at a minute area on the target in a spatial scale of interatomic distances in an instant of traversing interatomic distances. The spatiotemporally concentrated atomic collisions cause nonlinear effects in the kinetic energy loss processes of the molecular and cluster ions.

The first investigation of transmission of H_2^+ ions in carbon foils was reported by Poizat and Remillieux [1]. Brandt *et al.* [2] performed the first measurements of the energy loss from 60 keV/atom to 100 keV/atom of H_2^+ and H_3^+ ions passing through carbon and gold foils. Several groups [3–8] performed similar experiments using small cluster ions. Recently, the energy loss of such larger swift cluster ions as H_n^+ $(2 \leqslant n \leqslant 25)$ [9], B_n^+ $(2 \leqslant n \leqslant 4)$ [10], and C_n^+ $(2 \leqslant n \leqslant 8)$ [11,12] passing through thin foils have been measured. In these cases, the nonlinear effects associated with the energy loss processes were derived from the stopping power ratio defined as a ratio of the stopping power per atom of cluster ions to the stopping power of single atomic ions at the same velocity. The stopping power ratios, larger than unity at higher energies and less than unity at lower energies, have been derived in these measurements. Many theoretical studies have been performed to explain the nonlinear effects. These studies suggested that the nonlinear effect is the result of interference between the excitation of the target electrons and the simultaneous interaction with the cluster constituents in short internuclear distances [2,13–16]. This nonlinear effect was termed the "vicinage effect." Many experimental investigations for the nonlinear effects have been concentrated on the energy loss of swift cluster ions in the velocity region higher than the Bohr velocity.

On the other hand, very few experimental investigations in the region of the lower velocity than the Bohr velocity for the nonlinear effects have been performed on the energy loss of the slow cluster ions composed of heavy elements.

In this paper we present results of the energy loss measurements of slow C_n^+ $(2 \leqslant n \leqslant 21)$ cluster ions impinging at energies of 1.5–40 keV/atom on 1.0–10.0 $\mu g/cm^2$ thin-carbon-foil targets. The corresponding impinging velocities were 7%–36% of the Bohr velocity, the velocity region where the nuclear stopping power S_n of monoatomic carbon ions gradually decreases and the electronic stopping power S_e alternatively becomes dominant as the velocity increasing. We investigated the nonlinear effects on the energy losses at the lower velocity region for C_n^+ $(2 \leqslant n \leqslant 21)$ cluster-ion impacts.

II. EXPERIMENTAL METHOD

We used an electron impact-type cluster ion source which generated dominantly fullerene C_{60} cations such as C_{60}^{1+} (8.4 nA), C_{60}^{2+} (4.5 nA), C_{60}^{3+} (1.9 nA), and C_1^{1+} (10.9 nA), while the product abundances of different sizes of smaller carbon cluster ions were very few. The different sizes of smaller carbon cluster ions were produced only by fragmentation of the fullerene C_{60} cations downstream of the beam line. The experimental layout of the apparatus is illustrated in Fig. 1. The electron impact type ion source and a 45° sector-type analyzer magnet were mounted on the high voltage terminal. The C_{60} cations generated from the ion source were extracted by an extraction electrode. The C_{60} cations were selected by the first 45° analyzer magnet and then accelerated up to 100 kV through an acceleration column. The C_{60} ions were focused on a detector installed at 120 mm behind the target position in the scattering chamber using a three-run electrostatic quadrupole lens. The mass spectrometry and the energy spectrometry of the accelerated C_{60} ions were performed using the 15° sector-type second analyzer magnet. We detected various sizes of smaller carbon cluster ions produced by fragmentation of the C_{60} parent ions [17] in the scattering chamber. The C_n^+ cluster products in

*Corresponding author. Telephone: +81-3-5734-3055; Fax: +81-3-5734-2959; Electronic address: yasu.takahashi@aist.go.jp

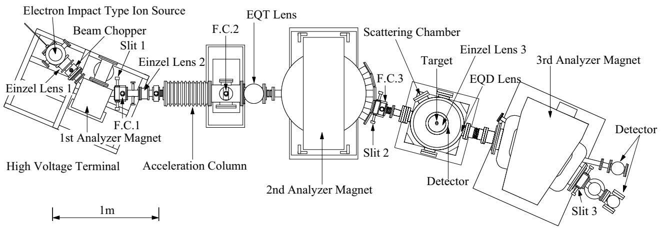

FIG. 1. Experimental setup for generation and acceleration of the carbon cluster ions. The energy losses of the cluster ions propagated through carbon foils of 1.0–10.0 μg/cm^2 in thickness were analyzed using the third 20° analyzer magnet.

smaller size of $n=2-30$ were consisted of both an even and odd number of carbon atoms, while in larger size $n=30-60$, only the even number products appeared. The single-charged ions in the smaller size were observed at the energies distributed around 80% of the C_{60} parent ions. The smaller cluster ions with energies lower than the full-accelerated energy were generated by fragmentation of the parent ions in the acceleration process. In contrast, the larger cluster ions exhibiting the same charge-state distribution as the C_{60} parent ions appeared at the full-accelerated energies. These cluster ions originated from the C_2-loss processes of the parent cluster ions in the after-acceleration processes [17]. The smaller C_n^+ cluster ions with the sizes $n=2$, 3, 5, 10, 13, 17, and 21 were used in the energy loss measurements.

Self-supported amorphous carbon foils of 1.0, 3.0, 5.0, and 10.0 μg/cm^2 thickness were prepared as targets in the experiments. The thickness of the foils was determined by measurement of the spectrophotometric absorption and transmission of a 340 nm ultraviolet ray. The deviation of uniformity in thickness of the carbon foils was less than 10%. Carbon foils of 1.0 μg/cm^2 thickness were only too thin to stand self-supportably in fabrication. The 1.0 μg/cm^2 carbon foil was supported by a stainless steel mesh of 0.32 mm $\times$0.32 mm size to mount on the target frame with an aperture of 10 mm in diameter. The transmissivity of the stainless steel mesh was 70.9%. The surfaces of the carbon foils were imaged using an optical microscope. On the 1.0 μg/cm^2 carbon foil, some cavities of several μm in diameter were opened through whole thickness. The target frames equipped with the 1.0–10.0 μg/cm^2 carbon foils were set on a movable target holder together with a blank target frame. The movable target holder was installed vertically with respect to the beam axis in the scattering chamber.

The third 20° analyzer magnet was set at 1027 mm far from the target for energy and mass analysis of cluster ions after transmission through the target carbon foil. Supposing the charge and the mass of the transmitted cluster ions are invariant, the energy loss ΔE of the intact cluster ion can be described as

$$\Delta E = E_0 - E_1 = E_0\left[1 - \left(\frac{B_1}{B_0}\right)^2\right], \tag{1}$$

where B_0 is the relative magnetic field corresponding to the incident energy E_0 of the primary beam, B_1 is the relative magnetic field corresponding to the energy E_1 after transmission of the intact cluster ion. The stopping power S of the intact cluster ion can be described as

$$S = \frac{\Delta E}{\Delta x} = \frac{E_0}{\Delta x}\left[1 - \left(\frac{B_1}{B_0}\right)^2\right], \tag{2}$$

where Δx is the thickness of the carbon foil. It is necessary to derive the stopping power per atom for quantitative discussion of the nonlinear effect on the stopping power of the intact cluster ion. The stopping power per atom S_1 of the cluster ion in consisting of n atoms can be described as

$$S_1 = \frac{1}{n}\frac{\Delta E}{\Delta x} = \frac{1}{n}\frac{E_0}{\Delta x}\left[1 - \left(\frac{B_1}{B_0}\right)^2\right]. \tag{3}$$

The relative magnetic fields B_0 and B_1 can be determined as peak positions in the energy spectra obtained by scanning the magnetic field.

The energy of the primary beams was measured by setting the blank target frame with an aperture of 10 mm in diameter on the primary beam axis. In the case of the 1.0 μg/cm^2 carbon foil, the energy of the primary beam was measured through the target frame aperture equipped with the blank stainless steel mesh. At the next step, the target frame equipped with the carbon foils was placed on the beam axis. The energy of the transmitted cluster ions was measured through the target foils. The energy measurements of the primary beam and the cluster ions were performed under the condition of the identical target holder except for the existence of carbon foils.

The analyzed cluster ions were detected using a secondary electron multiplier CERATRON (EMT-6081B, MURATA). The energy losses of the C_1^+ atomic ions with the same velocities were also measured. The output signals from the CERATRON were amplified by a pre-amplifier (109A, ORTEC) to discriminate against the noise level, and then accumulated by a count rate meter (449, ORTEC) after amplification using a main amplifier (435A, ORTEC).

III. EXPERIMENTAL RESULTS

We measured the energy losses of 1.5–40 keV/atom slow C_n^+ $(2 \leqslant n \leqslant 21)$ cluster ions propagated through 1.0–10.0 μg/cm^2 thin carbon foils. The velocities of the cluster ions employed in the experiments were less than the Bohr velocity. Charged particles were only detected after passing through the thin carbon foils, whereas no neutral particle was observed in the experiments. The energy spectra of the 80 keV C_2^+, C_5^+, and C_{13}^+ cluster ions analyzed by the third analyzer magnet are shown in Fig. 2. Figures 2(a)–2(c) are the energy spectra of the primary beams through the target frame aperture equipped with the blank stainless steel mesh. Figures 2(d)–2(f), are the energy spectra of the cluster ions transmitted through a 1.0 μg/cm^2 carbon foil. Two peaks were observed in the energy loss measurements. The first peaks located at the same energy position as the primary beam exhibit no energy loss due to passing cavities through the whole thickness. The second peaks located at the lower-energy position than the primary beam exhibit energy loss due to propagation through the carbon foil. We also observed

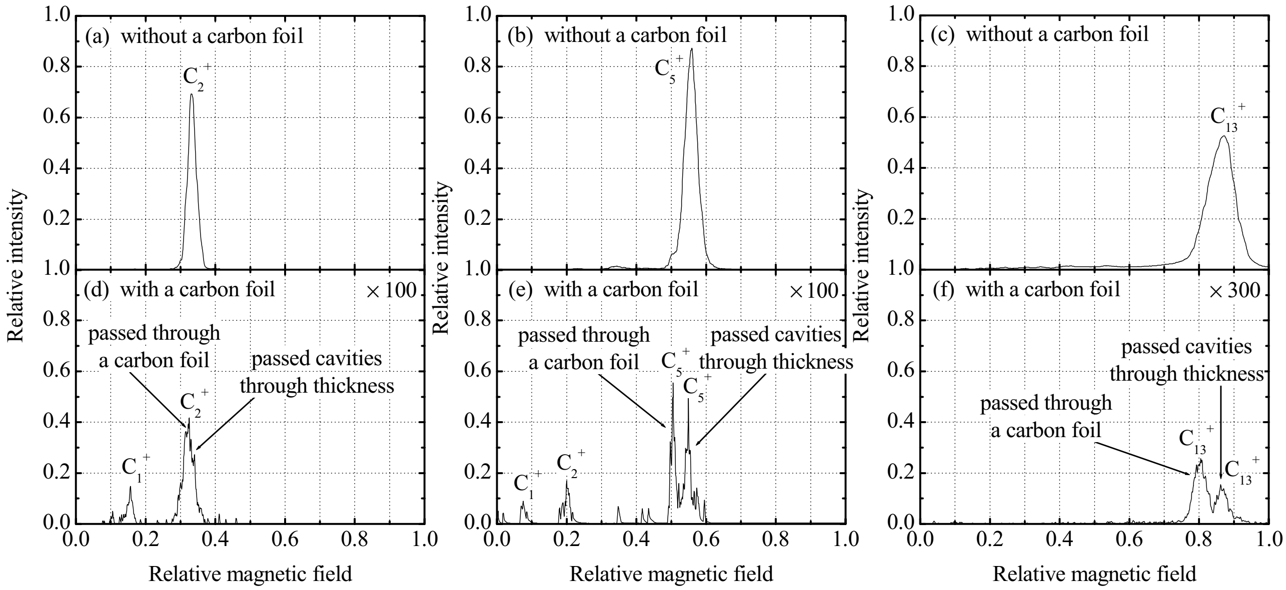

FIG. 2. Energy spectra of the 80 keV C_2^+, C_5^+, and C_{13}^+ cluster ions. (a), (b), and (c) are the energy spectra of the primary beams through the aperture equipped with a stainless steel mesh. (d), (e), and (f) are the energy spectra of the cluster ions transmitted through a 1.0 $\mu g/cm^2$ carbon foil. The energy losses and the stopping powers of the intact cluster ions were obtained from the averaged relative magnetic field at the peak positions in the two energy spectra, i.e., the primary beam and the intact cluster ions propagated through the thin foils.

single-charged fragment ions produced in the carbon foil. Most of the incident cluster ions were broken up in the carbon foil. However, we observed a small amount of intact cluster ions transmitted through the carbon foil. The intensities of the intact cluster ions and the fragment ions were below 1% of those of the primary beam. The intensities were reduced to a further lower level in the cases of the lower incident energies.

The energy spectra were measured five times in the cases of the blank target and the in-foil target, respectively. The energy spectra of the intact cluster ions through the foil exhibit a clear sharp peak to determine the relative magnetic fields corresponding to the peak positions. The relative magnetic fields B_0 and B_1 were derived from the mean values of the peak positions in the five spectra data. The peak positions in the five energy spectra data of the intact cluster ions through the blank aperture distributed with a narrow width of ±0.5% around the mean values, whereas the peak positions in the five energy spectra data of the intact cluster ions through the foil distributed with a wider width of ±3%. The mean FWHM (full width at the half-maximum) of the energy spectra of the intact cluster ions through the blank aperture was 4.8% of the peak energy, whereas the mean FWHM of the through-foil energy spectra was 2.2% of the peak energy. The energy losses and the stopping powers of the cluster ions in the foil were derived from Eqs. (1)–(3), using B_0 and B_1. The error of energy loss, ΔE was ±7% due to the error of B_0 and B_1 derived from the mean values of the five spectra data.

Following Eq. (2), the energy losses and the stopping powers of the intact cluster ions were given by the relative magnetic field at the peak position of respective energy spectra in Fig. 2 of the primary beam and the intact cluster ions transmitted through the thin foils. The energy losses and the stopping powers of the C_1^+ atomic ions at the same velocities were also obtained in the same way. The nonlinear effect of the stopping power of the C_n cluster, consisting of n atoms, was expressed by the stopping power ratio, which is defined as the stopping power per atom of the C_n cluster ion divided by the stopping power of the C_1 monoatomic ion at the same velocity:

$$R = \left(\frac{dE}{dx}\right)_{C_n} \Bigg/ n\left(\frac{dE}{dx}\right)_{C_1}. \qquad (4)$$

If the stopping power ratio is different from unity, the stopping power of the C_n cluster should contain a cross term besides a linear combination of the monatomic stopping power. We call the cross term a "nonlinear term" associated with the cluster system. Figure 3 is the stopping power ratios of the C_n^+ $(2 \leq n \leq 21)$ cluster ions transmitted through a 1.0 $\mu g/cm^2$ carbon foil. All stopping power ratios in any cluster size from $n=2$ to $n=21$ were less than unity. Remarkable nonlinear effects in the stopping power of the cluster ions were observed in the low-energy region from 1.5 keV/atom to 40 keV/atom. In the cluster-size dependence of the nonlinear effects, one should first pay attention to the fact that the stopping power ratios of C_2^+ were extremely small as $R \approx 0.25$ independent of the energy. The C_3^+–C_{10}^+ ions exhibited an increment in the stopping power ratio with the energy compared to C_2^+. A slight decrease was observed in C_{17}^+–C_{21}^+ although it did not appear clearly.

The intensities of the intact cluster ions and the fragment ions transmitted through the carbon foils decreased considerably as the foil becomes thicker. No transmission without fragmentation of the larger cluster ions, such as C_5^+–C_{21}^+, through the foils thicker than 1.0 $\mu g/cm^2$ was observed. The decrease of the fragment ions was based on enhancement of the scattering angles after passing through the foils. Another

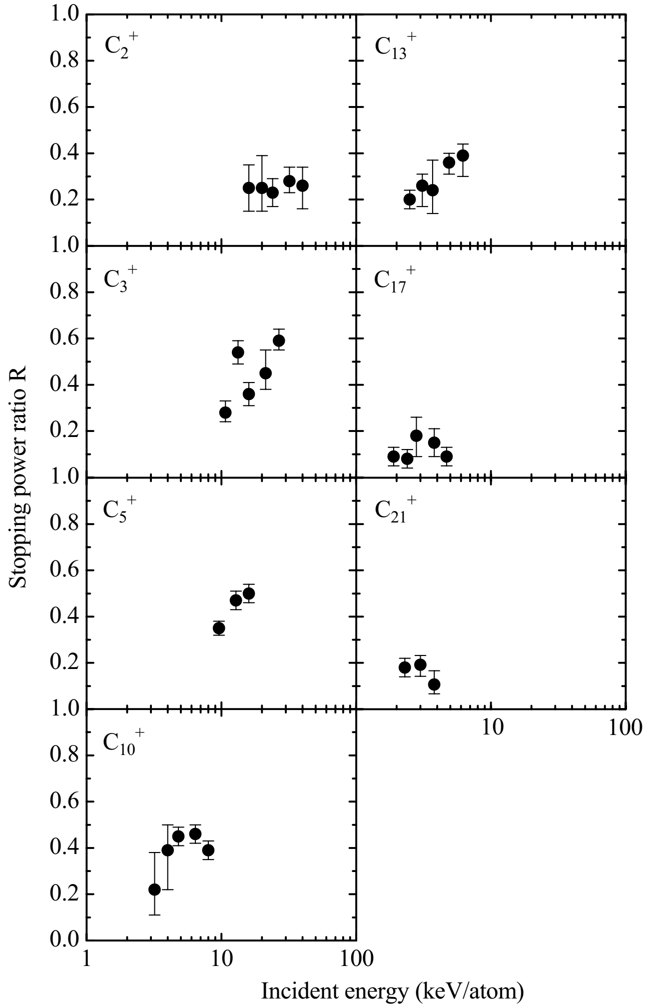

FIG. 3. Stopping power ratios of the C_n^+ ($2 \leqslant n \leqslant 21$) cluster ions propagated through a 1.0 μg/cm^2 thin carbon foil. The stopping power ratio was defined as the stopping power per atom of the cluster ion divided by the stopping power of the single atomic ion at the same velocity.

cause was the neutralization by electron capture in the foils at the low incident energies. In Fig. 4, the stopping power ratios of the 80 keV C_2^+ and C_3^+ ions without fragmentation are plotted as a function of foil thickness. The stopping power ratios of C_2^+, extremely low for the 1.0 μg/cm^2 carbon foil, rose with an increase in the foil thickness. The stopping power ratios of C_3^+ were almost constant relative to C_2^+, although there were a few variations in the experimental data.

IV. DISCUSSIONS

The nonlinear effects in the energy loss processes of the cluster ions seem to be the result of correlated motions among the cluster constituents while passing through a solid. The correlated motions among the charged particles passing through a free electron gas can be theoretically described [15] using the dielectric formalism derived by Lindhard [18]. This states that a medium is characterized by a dielectric

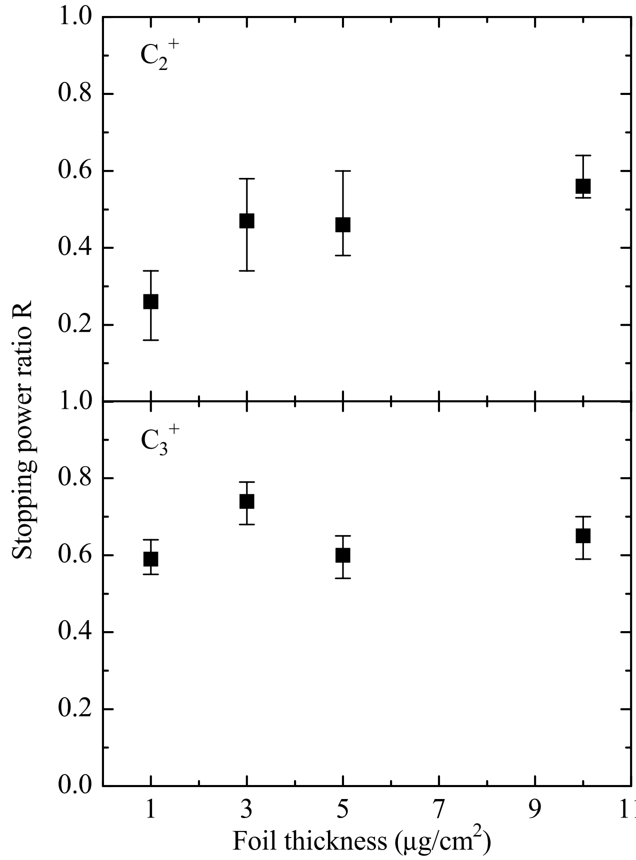

FIG. 4. The stopping power ratios of the 80 keV C_2^+ and C_3^+ cluster ions without fragmentation are plotted as a function of the foil thickness from 1.0 μg/cm^2 to 10.0 μg/cm^2.

function $\varepsilon(k,\omega)$ that depends on the momentum k and the energy ω transferred to the target electrons. The electronic stopping power of a cluster, which is isotropic and consists of n atomic ions with the charges $Z_i e$, can be written as

$$S_n = \sum_{i=1}^{n} S_i + \sum_{i \neq j} I_{ij}(r_{ij}). \quad (5)$$

The first term in Eq. (5) is a sum of the stopping powers S_i of the isolated atomic ions. S_i can be described using the dielectric formalism as

$$S_i = \frac{2Z_i^2 e^2}{\pi v^2} \int_0^\infty \frac{dk}{k} \int_0^{kv} d\omega\omega \, \mathrm{Im}\left[\frac{-1}{\varepsilon(k,\omega)}\right]. \quad (6)$$

The last term $I_{ij}(r_{ij})$ in Eq. (5) is an interference term that describes the "vicinage effects" of the spatial correlations among the cluster constituents. It can be written as

$$I_{ij}(r_{ij}) = \frac{2Z_i Z_j e^2}{\pi v^2} \int_0^\infty dk \frac{\sin(kr_{ij})}{k^2 r_{ij}} \int_0^{kv} d\omega\omega \, \mathrm{Im}\left[\frac{-1}{\varepsilon(k,\omega)}\right], \quad (7)$$

where r_{ij} represents the internuclear distance between the atomic ions ith and jth. The nonlinear effects are caused when the internuclear distances among the cluster constituents are short, since the electronic stopping power of the cluster ion is influenced by the interference term that expresses the interferences of the excitations of the target electrons.

Generally, in the high velocity region the cluster constituents lose their bound electrons through electronic interactions when a swift cluster enters a solid. The internuclear distance between each ion increases as the cluster travels through the solid due to the Coulomb repulsion. The cluster constituents act as isolated atomic ions because the correlation among each ion is gradually lost. Therefore, when a swift cluster enters a thin foil, the nonlinear effects are significant because of the short internuclear distances between the cluster constituents. The interference term $I_{ij}(r_{ij})$ in Eq. (5) greatly influences the electronic stopping power of a cluster. As the foil thickness is increased, the internuclear distances between the cluster constituents increases by the Coulomb explosion. The contribution of the interference term $I_{ij}(r_{ij})$ in Eq. (5) gradually loses relevance. The dependence between the foil thickness and the nonlinear effects has been observed in other energy loss measurements [9,10].

In this study, we derived the energy loss of the slow cluster ions from the intact cluster ions that were transmitted through a thin foil rather than from the fragment ions. Therefore, the internuclear distances between the cluster constituents were considered short and relatively constant in propagation through thin foils. It seems that the nonlinear effects in the energy loss processes are significant because of the strong correlation between the cluster constituents. For such correlations among the cluster constituents, the experimental results were qualitatively evaluated using a simplified united-atom model. In this model, a cluster that passes through a solid is regarded as a single atom. The single atom has an infinitesimal internuclear distance between the cluster constituents. For the detail of the model, one can refer to [19,20]. Briefly, the model assumes that the internuclear distances between the cluster constituents that pass through a solid are infinitesimally small. Thus, the spatial configuration of the cluster constituents is not taken into account. Furthermore, the charge state in solids is represented using a rough approximation. The charge state of a heavy ion in a solid is an important physical quantity. When the cluster ions are composed of heavy ions, the charge states in solids are lower than those of individual atomic ions at the same velocity [21,22]. Therefore, the charge states of cluster ions in solids cannot be neglected in the energy loss process. In the united-atom model, the charge state of a cluster is assumed to be equal to the charge state of a united atom. Sigmund *et al.* qualitatively derived the stopping power ratios that incorporate the concept of the effective charge of a single atomic ion with an atomic number Z to the united-atom model with the atomic number nZ [19]. The authors give an approximation for the stopping power ratio:

$$R = n\left(\frac{1-\exp\{-v/(nZ)^{2/3}v_0\}}{1-\exp\{-v/Z^{2/3}v_0\}}\right)^2, \tag{8}$$

where $v_0Z^{2/3}$ is the Thomas-Fermi velocity. When the united-atom model is applied, a decrease in the stopping power ratio is expected in the low velocity regions because of the low effective charge. Alternatively, an increase in the stopping power ratio is expected in the high velocity region because of the high effective charge. Both the increase and decrease effects in the stopping power ratio are significant at the limits of both velocity regions. The effects also depend significantly on the number of cluster constituents n. The united-atom model can predict the general behavior of the stopping power ratios derived from some experiments [20].

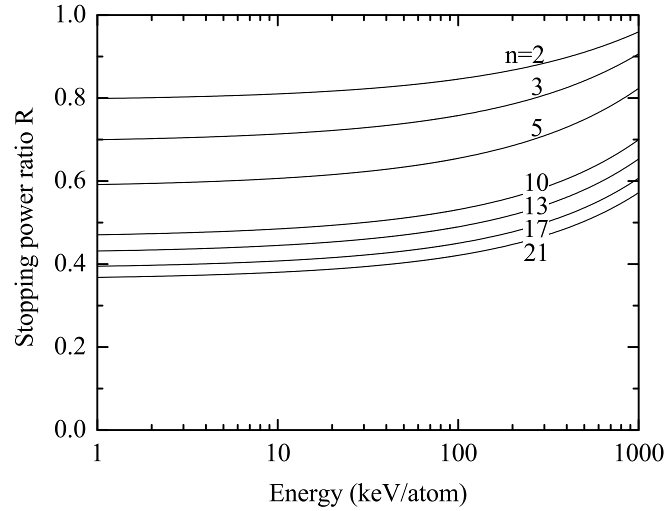

FIG. 5. Stopping power ratios of the C_n^+ ($2 \leqslant n \leqslant 21$) cluster ions obtained from the united-atom model in the low-energy region. These stopping power ratios were calculated using Eq. (8) for the energy per carbon atom E (keV/atom) of the C_n^+ cluster ion consistent with the experimental conditions. The number of cluster constituents n is given in each curve.

When the internuclear distances between the cluster constituents are assumed to be short in this simple united-atom model, both the spatial correlations and the charge states are taken into account as a limit of the correlation of the cluster constituents. Figure 5 is a plot of the stopping power ratios calculated using Eq. (8) of the C_n^+ cluster ion as a function of energy E (keV/atom) in the low-energy region. In the calculation, we used the parameters $2 \leqslant n \leqslant 21$, $Z=6$, $v_0 = 2.19 \times 10^6$ (m/s), and $v = (1.606E)^{1/2} \times 10^5$ (m/s). In the low energy region, the united-atom model qualitatively predicts that the stopping power ratios decrease below unity and then gradually approach unity as the incident energy increases. Moreover, the model predicts that the stopping power ratios decrease as the number of the cluster constituents increases. The result of the analytical approach is a rough correlation with the experimental results in Fig. 3, the stopping power ratios of the C_n^+ cluster ions propagated through a 1.0 μg/cm^2 carbon foil. However, the experimental results of the stopping power ratios are much smaller than the theoretical values obtained by the united-atom model. Relatively small values in the stopping power were observed in C_2^+, C_{17}^+, and C_{21}^+ cluster ions. In particular, the stopping power ratios of C_2^+ $R \approx 0.25$ in experiment are significantly different from the theoretical results $R \approx 0.8$. The experimental data indicating the foil-thickness dependence of the stopping power ratios of C_3^+ in Fig. 4 become almost in agreement with the theoretical results as the foil thickness increasing. However, significant disagreement between the theoretical and the experimental values still appear in the C_2^+ data in Fig. 4. In the energy loss processes of the slow cluster ions in a low-energy regime, it is necessary to take into account the effects of elastic collisions as well as the electronic interactions. The comparison between more detailed experiments and theories should be conducted for the energy losses of slow cluster ions passing through thin foils.

V. CONCLUSIONS

We measured the energy losses of slow C_n^+ $(2 \leq n \leq 21)$ cluster ions in the low-energy region at 1.5–40 keV/atom, where the velocities of the cluster ions are lower than the Bohr velocity. For all cluster sizes, we observed a certain low amount of intact cluster ions propagated through a very thin 1.0 $\mu g/cm^2$ carbon foil. Propagating through the foils thicker than 1.0 $\mu g/cm^2$, no larger C_n^+ $(5 \leq n \leq 21)$ cluster ion without dissociation was observed. The nonlinear effects in the energy loss process were derived using the stopping power ratio, defined as the ratio of the stopping power per atom of the cluster ion to the stopping power of the single atomic ion at the same velocity. The stopping power ratios of the intact cluster ions in all cluster sizes were much smaller than unity. The authors found the remarkable nonlinear effects in the low-energy region to be contrary to those predicted previously for the stopping power of the cluster ions. The stopping power ratios of the intact cluster ions propagated through the thin 1.0 $\mu g/cm^2$ carbon foils were qualitatively evaluated using the simplified united-atom model. In the low-energy region, the simple model qualitatively predicts a decrease in the stopping power ratios as the number of cluster constituents increases. The simplified united-atom model can be employed to obtain a rough estimate of the stopping power ratio behavior. However, the stopping power ratios of the C_2^+ clusters observed in the experiments were much smaller than unity beyond the values calculated by the model. The disagreement with the united-atom model in the dependence on the number of the cluster constituents was most significant in C_2^+ cluster ions.

[1] J. C. Poizat and J. Remillieux, Phys. Lett. **34A**, 53 (1971).

[2] W. Brandt, A. Ratkowsky, and R. H. Ritchir, Phys. Rev. Lett. **33**, 1325 (1974).

[3] J. W. Tape, W. M. Gibson, J. Remillieux, R. Laubert, and H. E. Wegner, Nucl. Instrum. Methods **132**, 75 (1976).

[4] J. C. Eckardt, G. Lantschner, N. R. Arista, and R. A. Baragiola, J. Phys. C **11**, L851 (1978).

[5] A. R. Nyaiesh, W. Steckelmacher, and M. W. Lucas, J. Phys. C **11**, 2917 (1978).

[6] R. Laubert, IEEE Trans. Nucl. Sci. **NS-26**, 1020 (1979).

[7] R. Levi-Setti, K. Lam, and T. R. Fox, Nucl. Instrum. Methods Phys. Res. **194**, 281 (1982).

[8] M. F. Steuer, D. S. Gemmell, E. P. Kanter, E. A. Johnson, and B. J. Zabransky, Nucl. Instrum. Methods Phys. Res. **194**, 277 (1982).

[9] E. Ray, R. Kirsch, H. H. Mikkelsen, J. C. Poizat, and J. Remillieux, Nucl. Instrum. Methods Phys. Res. B **69**, 133 (1992).

[10] K. Narumi, K. Nakajima, K. Kimura, M. Mannami, Y. Saitoh, S. Yamamoto, Y. Aoki, and H. Naramoto, Nucl. Instrum. Methods Phys. Res. B **135**, 77 (1998).

[11] K. Baudin, A. Brunelle, M. Chabot, S. Della-Negra, J. Depauw, D. Gardès, P. Håkansson, Y. Le Beyec, A. Billebaud, M. Fallavier, J. Remillieux, J. C. Poizat, and J. P. Thomas, Nucl. Instrum. Methods Phys. Res. B **94**, 341 (1994).

[12] Ch. Tomaschko, D. Brandl, R. Kügler, M. Schurr, and H. Voit, Nucl. Instrum. Methods Phys. Res. B **103**, 407 (1995).

[13] N. R. Arista and V. H. Ponce, J. Phys. C **8**, L188 (1975).

[14] J. Steinbeck and K. Dettmann, J. Phys. C **11**, 2907 (1978).

[15] N. R. Arista, Phys. Rev. B **18**, 1 (1978).

[16] N. R. Arista, Nucl. Instrum. Methods Phys. Res. B **164-165**, 108 (2000).

[17] Y. Takahashi, T. Hattori, H. Kashiwagi, T. Hata, and K. Yamamoto, Proceedings of the 2nd Union Symposium on Science Technology and Human, (Ionics Publish Co., LTD., Tokyo, 2003), Vol. 2, pp. 55.

[18] J. Lindhard, Mat. Fys. Medd. K. Dan. Vidensk. Selsk. **28**, 8 (1954).

[19] P. Sigmund, I. S. Bitensky, and J. Jensen, Nucl. Instrum. Methods Phys. Res. B **112**, 1 (1996).

[20] D. Ben-Hamu, A. Baer, H. Feldman, J. Levin, O. Heber, Z. Amitay, Z. Vager, and D. Zajfman, Phys. Rev. A **56**, 4786 (1997).

[21] D. Maor, P. J. Cooney, A. Faibis, E. P. Kanter, W. Koenig, and B. J. Zabransky, Phys. Rev. A **32**, 105 (1985).

[22] A. Brunelle, S. Della-Negra, J. Depauw, D. Jacquet, Y. Le Beyec, and M. Pautrat, Phys. Rev. A **59**, 4456 (1999).